Arch. Min. Sci. **71** (2026), 2, 177-198

Electronic version (in color) of this paper is available: http://mining.archives.pl

DOI: https://doi.org/10.24425/ams.2026.158812

KAMIL MUCHA[1*], ŁUKASZ BEDNAREK[1], JOANNA HYDZIK-WIŚNIEWSKA[1], IWONA JONCZY[2], JACEK NOWAK[2]

THE INFLUENCE OF MINERALOGICAL AND PETROGRAPHIC PROPERTIES ON THE ABRASIVITY AND ABRASIVENESS OF NATURAL STONES

The article discusses the relationship between mineralogical and petrographic properties and the wear resistance (abrasiveness) and abrasive characteristics (abrasivity) of natural stones. Abrasiveness is critical for the durability and functionality of these materials in construction applications. In contrast, rock abrasivity is assessed in the context of tool wear during stone processing. The research focuses on the mineralogical and petrographic characteristics of various types of natural stones, such as sandstones, granites, dolomites, and limestones, and their impact on the mechanical properties of these rocks. The article presents the results of laboratory tests that determine the degree of rock abrasivity and abrasiveness of natural stones, which is essential for selecting appropriate materials for specific construction purposes. The Böhme Abrasion Wheel Tester was used to assess rock abrasiveness, while the proprietary AGH abrasivity test was employed to evaluate rock abrasivity. The type of minerals within the stone's structure and the nature of the mineral binder directly affect the strength and abrasive properties of natural stones. The article also highlights the importance of material homogeneity and porosity in wear resistance.

Keywords: Rock abrasivity; rock abrasiveness; natural stone; cutting tools; wear

1. Introduction

Natural stone is a widely utilised material in the construction industry. However, before it can be used, it must first be extracted from a deposit. Not all deposits are suitable for exploitation, and not all rocks are suitable for the use as building materials [1]. The extraction of natural stone typically occurs at the surface in open-pit quarries. This process requires specialised machines

[1] AGH UNIVERSITY OF KRAKOW, AL. MICKIEWICZA 30, 30-059 KRAKÓW, POLAND
[2] SILESIAN UNIVERSITY OF TECHNOLOGY, 2 AKADEMICKA STR., 44-100 GLIWICE, POLAND

* Corresponding author: kmucha@agh.edu.pl

and equipment armed with cutting elements. The selection of cutting tools is often based on hardness, uniaxial compressive strength, and rock abrasivity [2]. These parameters influence the wear, specifically the abrasion of components that come into direct contact with the rock. During extraction, this includes cutting picks [3-5], drilling tools [6,7], bucket teeth [8,9], bulldozer blades, etc. (Fig. 1a). After extraction, the stone undergoes further processing, during which circular saw blades [10-12], wire saws [13,14], milling cutters [15,16], chisel picks [17], drill bits [18-20], and other tools are subjected to wear (Fig. 1b).

Mechanical wear is a phenomenon characterised by the loss of mass and changes in a tool's linear dimensions and shape caused by micro-cutting, scratching, and grooving [21]. Whether for extraction or processing, the wear process of tools incurs costs beyond the direct expenses of tool replacement. Each tool replacement results in machine downtime, thereby reducing its available operating time [16,22]. More frequent downtimes negatively impact the efficiency of the extraction or processing operation. Therefore, tools must be appropriately selected based on the specific properties of the rock being processed.

Properly cut and processed natural stone is used both indoors and outdoors. It can serve as paving stones, cladding panels, floor tiles, stair treads, and more (Fig. 2). However, for stone to be used as a finishing material, it must meet a range of specifications outlined in industry standards [27,28]. The primary property determining its suitability as paving stones is compressive strength [29], while for floor and stair tiles, bending strength is an additional critical factor [30]. Another essential characteristic of such stone is its resistance to environmental factors, including temperature fluctuations (frost resistance) [31] and rainfall (water absorption) [32,33]. Additionally, the stone's use on flat surfaces or staircases depends on its slip and abrasion resistance, which are vital as the material wears over time.

a)

b)

Fig. 1. Examples of wear on: a) working elements of extraction machinery, b) processing tools [23-26]

a) b) c)

Fig. 2. Examples of worn stone elements: a) sandstone doorstep, b) basalt paving stone, c) basalt and limestone slabs floor

Therefore, abrasive wear occurs at all stages: extraction, processing, and the use of natural stone. However, during the extraction and processing stages, the focus is on the abrasive wear of tools, where the rock's abrasivity is of interest. In contrast, during its use, the focus shifts to the abrasiveness of the natural stone [34].

The most widely used method for assessing rock abrasivity is the CERCHAR test [35], where the Cerchar Abrasivity Index (CAI) quantifies rock abrasivity. Researchers worldwide use this method to evaluate tool wear in rock-cutting tools. In the search for parameters influencing rock abrasivity, it is often correlated with other physical and mechanical properties, such as uniaxial compressive strength (UCS) [36,37], uniaxial tensile strength (BTS) [37,38], density [38,39], porosity [38,40], and even water absorption [41,42].

Research on the correlation between the Cerchar Abrasivity Index (CAI) and mineralogy and petrography dates back to the 1980s. Suana and Peters [43] demonstrated that a rock's quartz content significantly impacts the CAI value. Over the following years, many researchers confirmed this finding, although the focus was primarily on sandstones [2,44,45]. In rocks where quartz is not the predominant component, researchers began exploring the influence of other properties that affect rock abrasivity. Kahraman et al. [46] studied the impact of rock texture, Khoshzaher et al. [47] investigated the effect of grain size, and Jeong et al. [48] tested the influence of rock brittleness.

Although the Cerchar test is the most widely used for assessing rock abrasivity, it has generated considerable controversy. Rostami et al. [49] described how various parameters, such as pin hardness, scratching distance, test number, surface condition, and test speed, can influence the CAI value. As a result, the authors decided to evaluate rock abrasivity using a proprietary method developed at AGH University of Krakow in Poland [50].

The most commonly used method for assessing rock abrasiveness is the Böhme abrasion test. Strzałkowski et al. [51] presented the results of abrasiveness testing on several sandstones, analysing their petrographic properties, though the authors focused solely on the abrasiveness of one type of rock. In contrast, Mohammed et al. [52] analysed the abrasiveness of various types of rocks, attempting to correlate the results with physical and mechanical parameters rather than mineral composition. A similar analysis, considering bulk density and compressive strength, was conducted by Çobanoğlu & Çelik [53], who additionally demonstrated another abrasion testing method, the Wide Wheel Abrasion Test.

However, studies examining rocks' abrasivity and abrasiveness are rare [36,54]. Therefore, this article attempts to identify the relationship between abrasivity, abrasiveness, and mineralogical-petrographic properties. The study establishes what factors significantly influence the abrasive properties of rocks and the wear of the rock itself. Additionally, this article highlights the practical applications of research findings on the abrasivity and abrasiveness of natural stones used in the construction industry. Conducting a comprehensive set of tests can accelerate and optimise processes related to natural stone extraction and subsequent processing. It is also emphasised that selecting stone materials based on their abrasiveness is crucial for ensuring the durability and functionality of structures. Understanding the abrasiveness of stones enables engineers and architects to make informed decisions regarding materials that best meet the specific demands of construction projects.

2. Materials and methods

Four groups of natural stones were selected for the research, all commonly used in construction industry finishing works. These groups include sandstones, granites, limestones, and dolomites. The natural stones were sourced from various parts of Europe, primarily Poland, Germany, France, and Portugal. A profile of the tested materials and the exact location of the deposits is provided in TABLE 1.

TABLE 1

Tested natural stones

Scientific name	Location of the quarry, country	Rock code
Sandstone	Brenna, Poland	SB
Sandstone	Mucharz, Poland	SM
Sandstone	Żarnów, Poland	SZ
Sandstone	Barwałd, Poland	SBa
Granite	Strzegom, Poland	GS
Limestone	Celiny, Poland	LC
Limestone	Czatkowice, Poland	LCz
Limestone	Lompnes, France	LL
Limestone	Pêro Pinheiro, Sintra, Portugal	LP
Limestone	Nürnberg, Germany	LN
Dolomite	Libiąż, Poland	DL
Dolomite	Żelatowa, Poland	DZ

From each quarry, ten rock blocks were collected from the currently exploited area, each with a mass of approximately 10 kg. From each rock block, regular specimens with dimensions of 50×50×50 mm and 71×71×71 mm were prepared. All specimens were prepared according to the orientation of the extracted rock blocks. The preliminary selection included a macroscopic assessment of homogeneity and bedding. From each location, 25 cubic specimens with a side length of 50 mm and 10 cubic specimens with a side length of 71 mm were selected.

The investigations were conducted in accordance with the established research plan and the methodology described in Sections 2.1-2.4. These investigations included mineralogical and petrographic analysis as well as assessments of structural, strength and abrasive (abrasivity and abrasiveness) properties.

2.1. Petrographic and mineralogical analyses

Microscopic observations were carried out with transmitted light in thin sections using the OPTA-TECH LAB-40 HAL polarising diagnostic microscope equipped with an image analyser from the OPTA-TECH company.

The phase composition was determined using X-ray diffraction (XRD) on a D2 PHASER diffractometer from Bruker. The radiation source was a copper (Cu) lamp, operating at a voltage of 30 kV and a current of 20 mA during measurements. The interpretation of the obtained diffractograms was performed using the DIFFRAC.EVA v 6.1 software from Bruker and the PDF4 database.

The chemical composition was determined by X-ray fluorescence (XRF) using an S2 PUMA spectrometer from Bruker. The samples were crushed and homogenised for the measurements, then pressed in an automatic press under a pressure of 15 Mg. The measurements were conducted under a vacuum, using a silver (Ag) lamp to generate X-ray radiation.

2.2. Structural and strength properties analyses

As part of the evaluation of structural and strength properties, bulk density, open porosity, water absorption, and uniaxial compressive strength were conducted. The relevant standards performed all tests. The scope of the tests and the methods used are presented in TABLE 2. Each test was conducted on at least ten cubic samples with dimensions of approx. 50×50×50 mm. The results are presented as arithmetic means.

TABLE 2

Physical and mechanical properties and methods

Property	Standard	Description
Bulk density and open porosity	PN-EN 1936:2010 [55]	The tests were conducted using the hydrostatic method, which involves determining the volume of the samples by weighing them in water.
Water absorption	PN-EN 13755:2008 [56]	At atmospheric pressure, the samples were saturated to a constant mass in a water bath.
UCS	PN-EN 1926:2007 [57]	The uniaxial compressive strength was measured using a standard testing machine with a 1.0÷1.5 MPa/s loading rate.

2.3. AGH abrasivity test

Rock abrasivity was assessed using an original method developed at AGH University of Kraków (Fig. 3a). The method involves evaluating the mass wear of a standard steel pin in contact with a rock sample, applying a constant normal force of 300 N, and moving in a uniform circular motion at 50 rpm for 8 minutes. The tests can be performed on cylindrical (core) or cubic samples (Fig. 3b). The parameter characterising the rock abrasivity is the abrasivity index W_z, defined as the ratio of the mass loss of the steel pin to the mass loss of the rock sample, calculated using the formula (1).

$$W_z = \frac{m_{pa}}{m_{pi}} = \frac{m_{pab} - m_{paa}}{m_{pib} - m_{pia}} \tag{1}$$

where:

W_z – abrasivity index,
m_{pab} – mass of testing pin before test, g;
m_{paa} – mass of testing pin after test, g;
m_{pib} – mass of rock sample before test, g;
m_{pia} – mass of rock sample after test, g.

The rock abrasivity assessment is based on the average value of the abrasivity index W_z, calculated from a minimum of five measurements. The rock under investigation is classified according to the classification provided in TABLE 3.

(a)

(b)

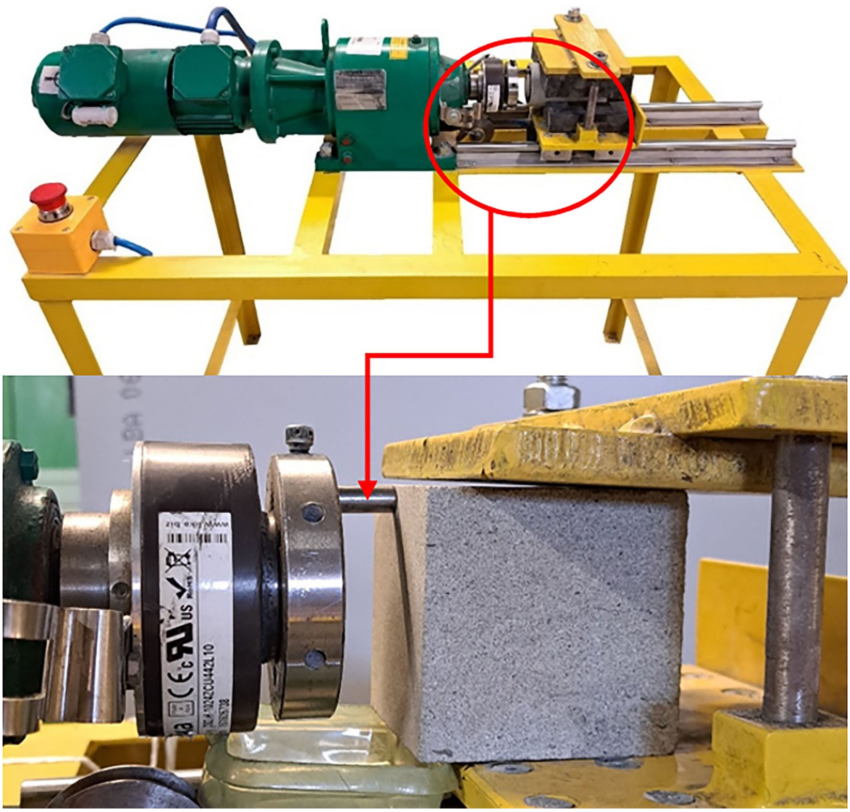

Fig. 3. AGH abrasivity test: (a) test stand, (b) friction pair

TABLE 3

Abrasivity classification using the AGH abrasivity test

Abrasivity index W_z [-]	Abrasivity
<0.1	negligible
0.1÷0.5	insignificant
0.5÷0.9	very low
1.0÷1.9	low
2.0÷2.9	medium
3.0÷3.9	high
4.0÷5.0	very high
>5.0	extreme

2.4. Böhme abrasion test

The abrasiveness of the tested natural stones was assessed using the Böhme Abrasion Wheel Tester (Fig. 4a) per the PN-EN 14157:2017-11 standard [58]. This method involves determining the wear of the rock sample due to abrasion on a rotating wheel made of cast iron using an abrasive material, specifically corundum powder. The samples subjected to testing are cubic, with an edge length of 71 (±1.5) mm, and are loaded with a force of 294 (±3) N. Each sample undergoes 16 abrasion cycles, each consisting of 22 revolutions. After each cycle, the wheel is cleaned, and a new portion of abrasive material is added. Additionally, the sample is rotated 90° around its axis to ensure uniform wear (Fig. 4b).

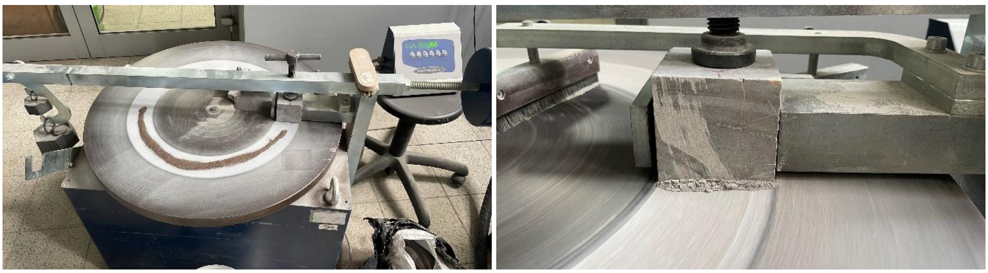

(a) (b)

Fig. 4. Böhme abrasion test: (a) test stand, (b) rock sample during the test

The assessment of abrasiveness is conducted on six samples, and the result is expressed as the average volume loss, calculated according to the formula (2).

$$\Delta V = \frac{\Delta m}{\rho_b} \tag{2}$$

where:

ΔV – sample volume loss after 16 cycles, mm^3;

Δm – sample mass loss after 16 cycles, g;

ρ_b – sample bulk density, g/mm^3.

3. Results

The tests were carried out following the previously established and above-described methodology. A mineralogical and petrographic analysis and the structural, strength and abrasive (abrasivity and abrasiveness) properties assessment were conducted for twelve natural stones.

3.1. Mineralogical and petrographic characteristic

Mineralogical and petrographic studies were conducted based on several research techniques, which enabled a comprehensive characterisation of the analysed rocks. TABLE 4 presents macroscopic photographs of the rocks alongside their microphotographs, showcasing the characteristic features of each rock in thin sections.

Sandstones are characterised by a psammitic structure, within which medium-grained sandstones (SB, SM, SBa) and fine-grained sandstone (SZ) can be distinguished. In all tested sandstones, the grains of the clastic material are well-rounded, with only sporadic occurrences of angular grains. The clastic material exhibits a low degree of sorting. The texture of the sandstones is chaotic and compact; however, differences among the sandstones are noticeable in the quantitative relationship between the clastic material and the binder. The binder of SB sandstone is porous, while a primary binder is also identified in the samples of SM and SBa sandstones. The binder of SZ sandstone can be described as contact-related, with some areas being porous. Based on observations in thin sections and using XRD analysis, it was determined that quartz predominates in the mineral composition of the clastic material in all sandstones, alongside feldspars (albite, orthoclase) and micas (muscovite, biotite). The binder comprises carbonate and clay minerals, with detailed identification facilitated by XRD analysis. According to the results, the mineral composition of the binder in sample SB identified calcite, which, along with dolomite and kaolinite, is also present in SM sandstone. In contrast, the binder of SBa sandstone consists of calcite, dolomite, illite, and kaolinite. Notably, only a quartz peak was observed in the XRD pattern of SZ sandstone.

Granite is characterised by a holocrystalline structure that is intermediate between medium-grained and fine-grained (with individual mineral crystals reaching approx. 1 mm in size), and it features a chaotic and compact texture. Its mineral composition includes quartz, plagioclase (albite), biotite, and opaque minerals, generally represented by magnetite.

The LC, LL, LP, and LN limestones exhibit a micritic structure, whereas LCz limestone is distinguished by a sparitic structure. The texture of all limestones is dense and chaotic. Their main constituents are carbonate minerals, which form a compact microcrystalline mass in microscopic images, where accumulations of iron oxides with a characteristic brown hue are often visible (except LL limestone). In thin sections of LCz limestone, small quartz grains were also observed, while the LN sample contained fragments of fossils, indicating an organic origin for the limestone. XRD analysis of samples LC, LL, LP, and LN revealed the presence of calcite with quartz admixtures. In contrast, in LCz limestone, the presence of calcite, quartz, dolomite, and clay minerals such as illite and kaolinite was identified.

The dolomites differ significantly in forming their mineral components; a dolosparitic structure characterises sample DL, while sample DZ has a dolomitic structure. Both rocks exhibit a dense and chaotic texture, with the DZ dolomite showing small caverns upon macroscopic observation. The mineral composition of samples DL and DZ is dominated by carbonate

TABLE 4

Mineralogical and petrographic description of tested natural stones

Stone code	Macro-photography	Microphotography*	Structure	Texture	Mineralogical composition**	SiO_2 [w.%]	Al_2O_3 [w.%]
1	**2**	**3**	**4**	**5**	**6**	**7**	**8**
SB		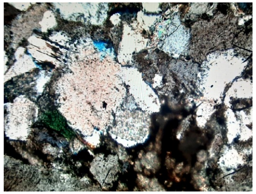	Psammitic, medium-grained sandstone	Dense and disorderly; porous binder	**Clastic material:** quartz, orthoclase, albite, muscovite, biotite. **Binder:** calcite, glauconite, kaolinite.	76.41	7.13
SM		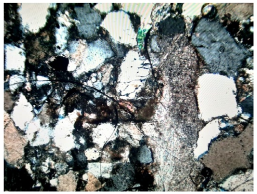	Psammitic, medium-grained sandstone	Dense and disorderly; basic binder	**Clastic material:** quartz, albite, muscovite, biotite. **Binder:** calcite, dolomite, kaolinite, glauconite.	45.09	7.81
SZ			Psammitic, fine-grained sandstone	Dense and disorderly; contact binder, porous in places	**Clastic material:** quartz, biotite. **Binder:** calcite.	95.77	1.75
SBa		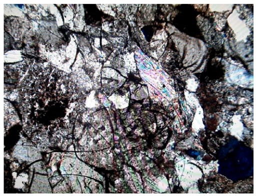	Psammitic, medium-grained sandstone	Dense and disorderly; basic binder	**Clastic material:** quartz, albite, muscovite, biotite. **Binder:** calcite, dolomite, illite, kaolinite.	56.71	7.54

TABLE 4. CONTINUED

1	2	3	4	5	6	7	8
GS		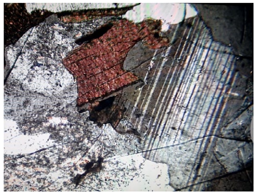	Full crystalline, borderline medium- and fine-crystalline	Dense and disorderly	Quartz, albite, microcline, biotite.	71.23	12.97
LC		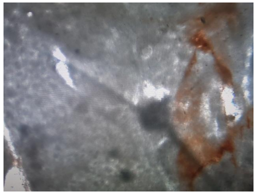	Mikritic	Dense and disorderly	Calcite, quartz.	1.21	0.29
LCz			Sparitic	Dense and disorderly	Calcite, dolomite, quartz, albite, illite, kaolinite.	40.52	8.35
LL		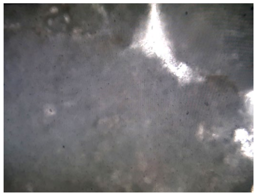	Mikritic	Dense and disorderly	Calcite, quartz.	0.53	0.24

TABLE 4. CONTINUED

1	2	3	4	5	6	7	8
LP		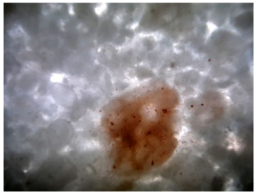	Mikritic	Dense and disor-derly	Calcite, quartz.	0.39	0.22
LN			Mikritic	Dense and disor-derly	Calcite, quartz.	1.05	0.34
DL			Dolosparitic	Dense and disor-derly	Dolomite, calcite, quartz, albite, illite.	46.2	10.14
DZ	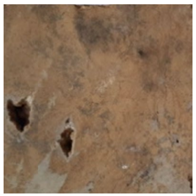		Dolomitic	Dense and disor-derly	Dolomite, calcite, quartz, albite.	0.62	0.30

* microphotographs in thin sections, crossed polarisers, magnification 100×
** mineral composition determined based on microscopic observations and XRD analysis

minerals alongside quartz, plagioclases, accumulations of iron oxides, and glauconite, with a characteristic green colour visible under parallel polarisers in sample DL. In sample DZ, small quartz grains and opaque minerals can be observed, as well as dispersed iron compounds with brown colouration. As noted during macroscopic observations, their presence as a pigment gives the rock a dark yellow tint. XRD studies indicated that in both analysed samples, the carbonates are represented by dolomite and calcite; additionally, sample DL contained quartz, albite, and illite.

3.2. Structural and strength properties assessment

The results of the evaluation of physical and mechanical properties, presented in TABLE 5, indicate a significant variation in the properties of the studied rocks depending on their geological formation.

The tested rocks can be classified based on their physical and mechanical properties. The rocks with the highest bulk density, exceeding 2600 kg/m^3 (SM sandstone, GS granite, and all limestones), also exhibit very low open porosity, with a maximum of 2.58% for SM sandstone and 2.39% for LN limestone. For the remaining limestones and granite, the values of open porosity ranged from 0.59% to 1.51%. Low open porosity results in deficient water absorption, not exceeding 1%. Notable differences are observed in the uniaxial compressive strength values. The rocks with the highest UCS are granites and limestones, excluding the LCz limestone. The UCS values range from 139.5 MPa (LC) to 190.9 MPa (LP). The UCS of LCz limestone, the SB, SM, and SBa sandstones, and DL dolomite ranges from 82.5 MPa (DL) to 123.4 MPa (SM). The rocks with the lowest strength properties are the SZ sandstone and the DZ dolomite, which have approximately a UCS 54 MPa. They also have the lowest bulk density, around 2000 kg/m^3, and high porosity (SZ – 15.20%, DZ – 24.04%).

TABLE 5

Physical and mechanical properties of tested natural stones

Rock code	Bulk density [kg/m^3]		Open porosity [%]		Water absorption [%]		UCS [MPa]	
	min-max	mean	min-max	mean	min-max	mean	min-max	mean
SB	2438-2475	2457	4.86-7.15	6.60	2.44-2.91	2.69	58.9-115.7	103.7
SM	2646-2681	2660	2.11-3.14	2.58	0.51-1.42	0.97	98.3-140.6	123.4
SZ	2019-2060	2039	12.63-18.74	15.20	6.72-7.93	7.40	39.0-69.4	54.2
SBa	2513-2662	2587	2.95-3.98	3.63	0.59-1.93	1.40	77.4-160.1	117.9
GS	2552-2680	2618	0.46-1.03	0.86	0.15-0.96	0.33	97.2-217.0	157.8
LC	2665-2678	2667	0.58-1.21	1.09	0.32-0.67	0.41	81.5-226.8	139.5
LCz	2683-2743	2696	0.36-0.76	0.67	0.15-0.31	0.25	95.1-138.4	112.7
LL	2683-2689	2686	0.32-0.61	0.59	0.14-0.28	0.22	107.1-200.5	149.5
LP	2642-2668	2656	0.98-1.87	1.51	0.42-0.81	0.57	106.3-241.6	190.9
LN	2581-2615	2598	2.14-2.54	2.39	0.69-1.24	0.92	138.0-162.6	148.2
DL	2399-2431	2413	3.97-5.16	4.95	1.02-3.13	1.98	72.1-96.9	82.5
DZ	1950-2120	2020	22.58-25.67	24.04	7.50-14.20	11.90	45.4-65.6	54.1

3.3. Abrasivity assessment

According to the previously mentioned method (the AGH abrasivity test) for assessing the rock abrasivity, in order to determine the value of the abrasivity index W_z, it is necessary to calculate the mass loss of the steel pin and the mass loss of the rock sample after each experimental trial. Five trials were conducted for each type of stone. TABLE 6 presents the minimum, maximum, and mean values for both the wear of the pins and the rock samples, from which the abrasivity index W_z was calculated. Each natural stone was then classified according to TABLE 3.

TABLE 6

Results of abrasivity assessment

Rock code	Mass loss of the steel pin [g]		Mass loss of the rock sample [g]		Abrasivity index W_z [-]		Abrasivity
	min-max	mean	min-max	mean	min-max	mean	
SB	0.21÷0.27	0.24	0.09÷0.10	0.10	2.24÷3.01	2.6	Medium
SM	0.10÷0.12	0.11	0.09v0.11	0.10	1.03÷1.33	1.1	Low
SZ	0.25÷0.29	0.27	0.51÷0.73	0.60	0.40÷0.50	0.5	Very low
SBa	0.17÷0.21	0.19	0.13÷0.15	0.14	1.19÷1.61	1.4	Low
GS	0.31÷0.35	0.34	0.07÷0.09	0.08	3.75÷4.21	4.0	High
LC	0.00	0.00	0.06÷0.09	0.08	0.00	0.0	Negligible
LCz	0.03÷0.04	0.03	0.38÷0.67	0.49	0.05÷0.08	0.1	Negligible
LL	0.00	0.00	0.12÷0.13	0.13	0.00	0.0	Negligible
LP	0.00	0.00	0.11÷0.13	0.12	0.00	0.0	Negligible
LN	0.00	0.00	0.13÷0.15	0.14	0.00	0.0	Negligible
DL	0.01÷0.02	0.01	0.34÷0.53	0.46	0.02÷0.05	0.0	Negligible
DZ	0.00	0.00	2.89÷3.43	3.20	0.00	0.0	Negligible

The GS granite exhibits the highest abrasivity index value, with a mean W_z value of 4.0, classifying it as a rock of high abrasivity. The SB sandstone is classified as a rock of medium abrasivity, with an abrasivity index of 2.6. The SB and SM sandstones are categorised as rocks of low abrasivity, both falling within the index range of 1.0 to 2.0. Among the tested sandstones, the SZ sandstone has the lowest abrasivity index of 0.5, classifying it as a rock of very low abrasivity. For both the limestones and dolomites, the abrasivity index is below 0.1, indicating that the abrasivity of these rocks is negligible.

However, it is essential to consider the value of the abrasivity index W_z and the mass loss values for the steel pin and the rock sample. Notably, the most significant mass loss for the steel pin was observed for GS granite, averaging 0.34 g. Interestingly, the second-highest average mass loss for the steel pin, equal to 0.27 g, was recorded for the SZ sandstone, classified as a rock with very low abrasivity. However, the SZ sandstone exhibited a significant mass loss for the rock sample, averaging 0.6 g, which is over seven times higher than the average mass loss of the GS granite sample. It indicates that while the SZ sandstone demonstrates good abrasive properties, potentially leading to faster wear of cutting or drilling tools, it is also a brittle rock. It has grains which easily break off, making it much easier to cut with than granite.

3.4. Abrasiveness assessment

TABLE 7 presents the results of the abrasiveness tests conducted using the Böhme Abrasion Wheel Tester for all twelve tested natural stones.

TABLE 7

Results of abrasiveness assessment

Rock code	Sample volume loss ΔV [mm^3]	
	min-max	**mean**
SB	27 221÷33 271	29 389
SM	21 676÷24 197	22 836
SZ	86 201÷87 209	86 856
SBa	22 685÷37 303	31 002
GS	10 082÷11 090	10 586
LC	10 082÷13 107	11 594
LCz	22 937÷23 390	23 088
LL	13 611÷20 668	16 383
LP	18 148÷19 660	18 702
LN	14 619÷18 652	17 139
DL	26 213÷37 959	31 355
DZ	42 849÷52 931	48 898

It can be observed that the SB, SM and SBa sandstones exhibit very similar abrasiveness. The reduction in volume resulting from abrasion for these three types of sandstone ranged from 22 836 to 31 002 mm^3. Notably, the results obtained for the SZ sandstone, which exhibited an abrasiveness of 86 856 mm^3, were the highest among all tested samples. Conversely, the GS granite demonstrated the lowest abrasiveness of all the examined rocks, with a value of 10 586 mm^3. In the case of the limestones, the abrasiveness values were quite similar. The most significant volume change due to abrasion was recorded for the LCz limestone (23 088 mm^3), while the lowest was for the LL limestone (16 383 mm^3). The DZ dolomite also exhibited relatively high abrasiveness at 48 898 mm^3.

4. Discussion

Few researchers have undertaken the exploration of the relationship between abrasiveness and abrasivity. Their investigations primarily employed simple regression and, less frequently, multiple regression. Deliormanlı [36] utilised simple linear regression to examine the relationship between abrasiveness on the Böhme Abrasion Wheel Tester and the abrasivity index (CAI) (Fig. 5a). In his publication, he stated that *there is a strong negative relationship is CAI and Bohme abrasion values* evidenced by a correlation coefficient of $R = -0.91$. Similarly, Teyman [54] also used simple regression to investigate the relationship between abrasiveness on the Böhme Abrasion Wheel Tester and the abrasivity index (CAI). In his case, as illustrated in Fig. 5b, the abrasiveness decreases with increasing CAI values. However, the coefficient of determination (R^2) was at a level of 0.67.

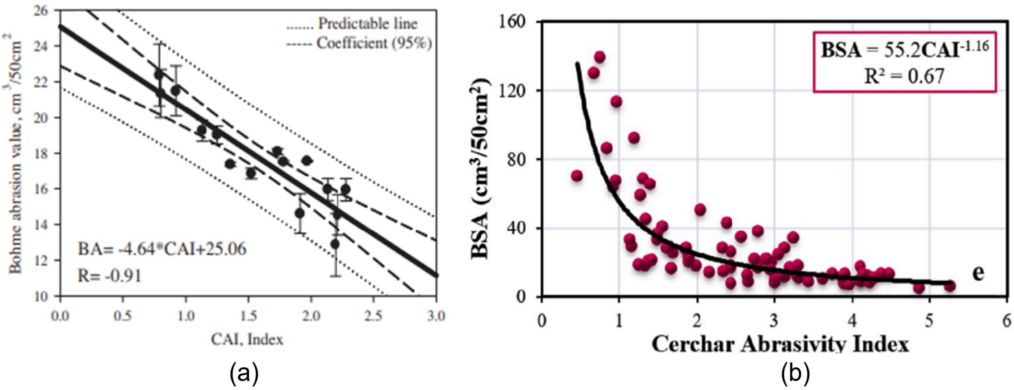

Fig. 5. Relationship between abrasivity and abrasiveness: (a) acc. to. Deliormanlı, (b) acc. to. Teymana [36,54]

The literature also includes attempts to explore the relationship between abrasivity and mineral composition, with a predominant focus on quartz. Ko et al. [37] used simple linear regression to investigate the relationship between the CAI value and the percentage content of quartz. The studies were conducted for two groups of rocks, igneous and metamorphic, yet their results were somewhat surprising. For both groups, the CAI value decreased as the percentage content of quartz increased. However, the coefficients of determination (R^2) were found to be at levels of 0.2 and 0.04, respectively. Similarly, Li et al. [59] sought to identify the relationship between abrasivity and the percentage content of quartz while additionally considering the grain size of quartz. Their research demonstrated that *the abrasivity increases with the rising of quartz size, and the different contents of quartz results in a different increasing rate.* However, it should be noted that these studies were conducted solely on sandstones and granites.

Gunes Yılmaz et al. [60] demonstrated similar relationships concerning rock abrasiveness. They found that the percentage of quartz content was the primary petrographic variable influencing the increased abrasion resistance of the studied granites. Moreover, a high correlation ($R^2 = 0.82$) was observed between the quartz-to-feldspar ratio and abrasiveness, where abrasion resistance increased as the ratio of quartz to feldspar increased.

As can be observed, the CAI abrasivity index is most commonly used for evaluating rock abrasivity. Nevertheless, in this study, an original proprietary method was applied to assess rock abrasivity, while the review of the above-mentioned studies and the analysis of the results presented therein were intended to support the selection of appropriate variables for the statistical analysis of the authors' own results.

Based on the results, the authors of this paper attempted to predict the abrasive properties (abrasiveness and abrasivity) of natural stones at various stages of their use. To achieve this, multiple regression analysis was applied, which allows the prediction of a given variable using several independent variables.

Initially, an attempt was made to predict rock abrasivity in natural stone extraction and processing. Since the abrasivity index W_z for several natural stones was zero (according to the classification in TABLE 3, abrasivity is considered negligible), these values were not included in the multiple regression analysis. For the prediction, three variables were taken into account:

uniaxial compressive strength (σ_c), silica content (SiO_2), and bulk density (ρ_b). This relationship can be described by Eq. (3).

$$W_z = 0.0539 * \sigma_c + 0.0354 * SiO_2 - 0.00264 * \rho_b \quad (3)$$

TABLE 8 presents the statistical values from the multiple regression analysis. Notably, the coefficient of determination (R^2) is 0.96, indicating a high degree of fit. In addition, the graphs (Figs. 6a-6c) display the abrasivity index values obtained from the experiments alongside the

TABLE 8

Multiple regression analysis for abrasivity

	Coefficients	**Standard Error**	**t Stat**	**P-value**	**Lower 95%**	**Upper 95%**	R^2
σ_c	0.053882	0.008851	6.087807	0.003681	0.029308	0.078455	0.96
SiO_2	0.035428	0.008936	3.964418	0.016616	0.010616	0.060239	
ρ_b	–0.00264	0.000501	–5.27417	0.006195	–0.00403	–0.00125	

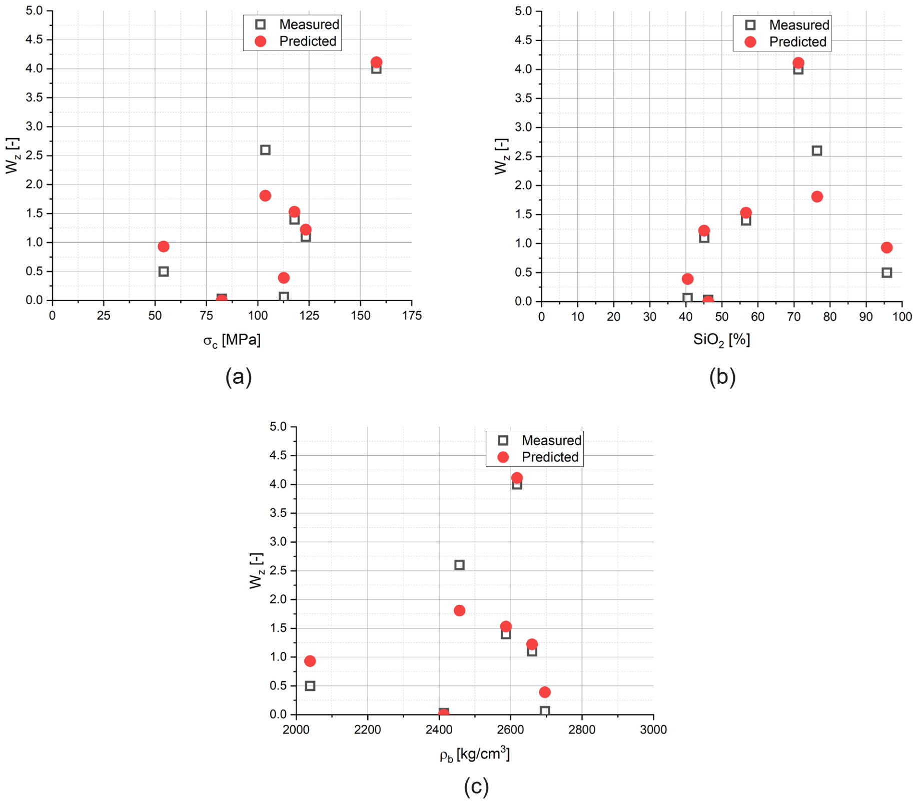

Fig. 6. The relationship between the observed and predicted abrasivity, considering the following factors: (a) uniaxial compressive strength, (b) silica content, (c) bulk density

predicted abrasivity index values for each variable included in the multiple regression analysis. The points representing the observed and predicted values do not significantly diverge from each other, further demonstrating the accuracy and reliability of the statistical analysis conducted.

The next stage involved predicting the abrasiveness of natural stone, which determines its suitability, particularly for flooring. A multiple regression analysis was applied again, where the primary factor considered was the abrasivity index W_z and the weight loss of the steel pin and the sample during the abrasivity testing. The goal was to estimate the stone's abrasiveness at the extraction and processing stages based on its abrasivity. Three different multiple regression trials were conducted, each using different factors:

- Trial 1: uniaxial compressive strength (σ_c), silica content (SiO_2), bulk density (ρ_b);
- Trial 2: weight loss of the steel pin (m_{pa}), weight loss of the rock sample (m_{pi});
- Trial 3: abrasivity (W_z), porosity (p), silica content (SiO_2).

The results and relationships obtained from these multiple regression trials are summarised in TABLE 9. Each trial yielded satisfactory results due to the high coefficient of determination values. However, trial 3 was the best, with $R^2 = 0.95$. Therefore, Eq. (4) provides the best prediction of the abrasiveness index value.

$$\Delta V = -8584.96 * W_z + 2142.126 * p + 572.35 * SiO_2 \tag{4}$$

For this trial, the relationships between abrasiveness and the individual factors considered in the third regression trial are illustrated in Figs. 7a-7c.

TABLE 9

Multiple regression analysis for abrasiveness

Trial 1							
$\Delta V = -432.78 * \sigma_c + 165.31 * SiO_2 + 29.48 * \rho_b$							
	Coefficients	**Standard Error**	**t Stat**	**P-value**	**Lower 95%**	**Upper 95%**	**R^2**
σ_c	–432.79	181.1121	–2.38962	0.040582	–842.494	–23.0855	0.83
SiO_2	165.3112	163.4345	1.011483	0.338204	–204.403	535.0258	
ρ_b	29.48336	10.27652	2.869002	0.018507	6.236253	52.73047	
Trial 2							
$\Delta V = 105750.2 * m_{pa} + 18675.56 * m_{pi}$							
	Coefficients	**Standard Error**	**t Stat**	**P-value**	**Lower 95%**	**Upper 95%**	**R^2**
m_{pa}	105750.2	35578.37	2.972319	0.01399	26476.7	185023.8	0.67
m_{pi}	18675.56	6764.962	2.76063	0.020108	3602.285	33748.83	
Trial 3							
$\Delta V = -8584.96 * W_z + 2142.126 * p + 572.35 * SiO_2$							
	Coefficients	**Standard Error**	**t Stat**	**P-value**	**Lower 95%**	**Upper 95%**	**R^2**
W_z	–8584.96	2884.71	–2.97602	0.01555	–15110.6	–2059.29	0.95
p	2142.126	369.4503	5.798143	0.00026	1306.371	2977.88	
SiO_2	572.3528	97.7427	5.855709	0.000242	351.2435	793.4622	

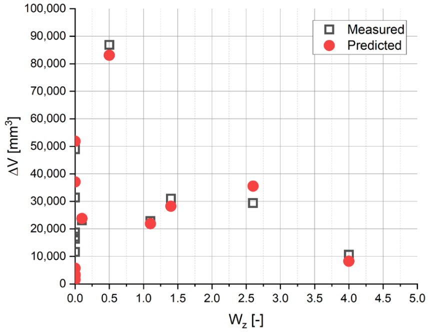

(a)

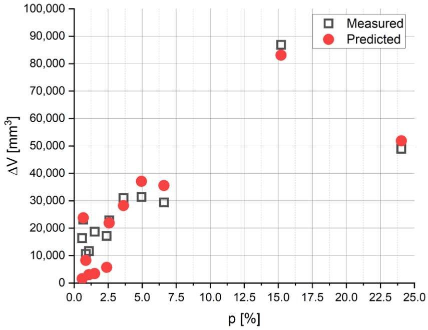

(b)

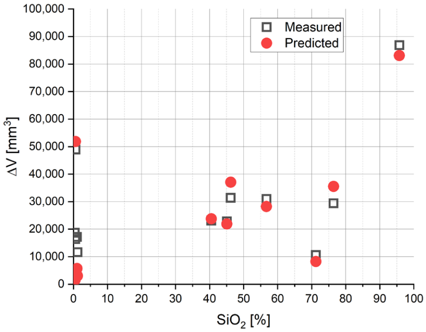

(c)

Fig. 7. The relationship between abrasiveness and the following factors: (a) abrasivity, (b) porosity, (c) silica content, for both measured and predicted values

5. Conclusion

The article analyses the influence of selected physical and mechanical properties as well as mineralogical-petrographic characteristics on the abrasive properties of natural stones. Twelve types of natural stones representing sandstones, granites, limestones, and dolomites were analysed.

The experimental results demonstrated a significant variability in the abrasive properties of the analysed rocks. To evaluate rock abrasivity, an original proprietary method was applied in which abrasivity is described by the W_z index (Eq. 1). Granites were characterised by the highest abrasivity, whereas sandstones exhibited moderate or low abrasivity depending on their mineral composition. In contrast, limestones and dolomites showed negligible abrasivity. With regard to abrasiveness, determined using the widely known Böhme method, the highest volume loss was recorded for sandstone, whereas the lowest abrasiveness was observed for granite. These results indicate that rocks may simultaneously exhibit low abrasivity and high abrasiveness, which is associated with their brittleness and the detachment of grains during the abrasion process.

Multiple regression analysis confirmed that the abrasive properties of natural stones can be effectively predicted using selected mineralogical and mechanical parameters. The abrasivity index was successfully modelled using uniaxial compressive strength, SiO_2 content, and bulk density, achieving a high coefficient of determination ($R^2 = 0.96$), which indicates a very good fit of the model. Similarly, abrasiveness can be predicted using several combinations of parameters. Among the tested models, the best results were obtained for the regression equation including abrasivity index, porosity, and SiO_2 content, for which the coefficient of determination reached $R^2 = 0.95$.

The most important achievement of this study is the development of relationships enabling the prediction of the abrasivity index W_z (Eq. 3) and abrasiveness ΔV (Eq. 4) based on basic rock properties and their mineralogical composition. The obtained models allow preliminary estimation of these parameters without the need for time-consuming laboratory tests. This may be particularly useful at the stage of selecting rock cutting methods and types of cutting tools, as well as during the preliminary assessment of the suitability of natural stones for specific practical applications.

The determined relationships may enable the optimisation of production processes, for example, through the application of appropriate cooling techniques and the use of tools with specialised protective coatings, which may increase the durability of cutting tools and consequently reduce energy consumption and operational costs. Proper interpretation of the derived relationships allows for a better understanding of the mechanisms of material wear and degradation, which is essential for improving the durability and reliability of products manufactured from these materials. For example, in construction or in the production of building materials, abrasion resistance is a key parameter determining the durability of finished products used, for instance, in flooring applications.

Additionally, this knowledge may also be applied in the design of new materials with specific mechanical properties. For example, the appropriate selection of mineral components may lead to the development of materials with increased wear resistance, which is important in many industrial sectors such as construction, road engineering, and the chemical industry.

References

[1] C. Schneider-Löbens, S. Siegesmund, K.J. Stein, S. Löbens, Joint analysis as an important tool for an optimizing block extraction of natural stones. Environmental Earth Sciences **81**, 94 (2022). DOI: https://doi.org/10.1007/s12665-022-10177-3

[2] I. Jonczy, K. Mucha, Relationships between the petrographic and abrasive properties of sandstones in the aspect of their cutting. Energies **15**, 2692 (2022). DOI: https://doi.org/10.3390/en15072692

[3] S. Dewangan, S. Chattopadhyaya, Characterization of wear mechanisms in distorted conical picks after coal cutting. Rock Mech. Rock Eng. **49**, 225-242 (2016). DOI: https://doi.org/10.1007/s00603-015-0726-x

[4] S. Liu, H. Ji, X. Liu, H. Jiang, Experimental research on wear of conical pick interacting with coal-rock. Engineering Failure Analysis **74**, 172-187 (2017). DOI: https://doi.org/10.1016/j.engfailanal.2017.01.013

[5] K. Kotwica, Atypical and innovative tool, holder and mining head designed for roadheaders used to tunnel and gallery drilling in hard rock. Tunnelling and Underground Space Technology **82**, 493-503 (2018). DOI: https://doi.org/10.1016/j.tust.2018.08.017

[6] M. Capik, A.O. Yilmaz, Correlation between Cerchar abrasivity index, rock properties, and drill bit lifetime. Arabian Journal of Geosciences **10**, 15 (2017). DOI: https://doi.org/10.1007/s12517-016-2798-7

[7] B. Jiang, F. Ma, Q. Wang, H. Gao, D. Zhai, Y. Deng, Ch. Xu, L. Yao, Drilling-based measuring method for the c-φ parameter of rock and its field application. International Journal of Mining Science and Technology **34**, 1, 65-76 (2024). DOI: https://doi.org/10.1016/j.ijmst.2023.06.005

[8] S. Singla, A.S. Kang, J.S. Grewal, G.S. Cheema, Wear behaviour of weld overlays on excavator bucket teeth. Procedia Materials Science **5**, 256-266 (2014). DOI: https://doi.org/10.1016/j.mspro.2014.07.265

[9] S. Kostić, J. Trivan, Optimization of Coal Overburden Excavation Considering Variable Geomechanical Properties and States of Excavator Teeth. Archives of Mining Sciences **61**, 1, 123-142 (2022). DOI: https://doi.org/10.24425/ams.2022.140706

[10] G. Aydin, I. Karakurt, K. Aydiner, Wear performance of saw blades in processing of granitic rocks and development of models for wear estimation. Rock Mech. Rock Eng. **46**, 1559-1575 (2013). DOI: https://doi.org/10.1007/s00603-013-0382-y

[11] J. Zhou, J. Zhang, H. Zhou, P. Dong, K. Wang, Wear characteristics of diamond segments on multi-blade combination saw with different diameters in granite sawing. International Journal of Refractory Metals and Hard Materials **97**, 105517 (2021). DOI: https://doi.org/10.1016/j.ijrmhm.2021.105517

[12] J. Kang, J. Zhang, K. Wang, D. Zhang, T. Bai, H. Zhang, W. Song, Analysis of wear mechanism and sawing performance of carbide and PCD circular saw blades in machining hard aluminum alloy. International Journal of Refractory Metals and Hard Materials **116**, 106362 (2023). DOI: https://doi.org/10.1016/j.ijrmhm.2023.106362

[13] M. Ataei, R. Mikaiel, F. Sereshki, N. Ghaysari, Predicting the production rate of diamond wire saw using statistical analysis. Arabian Journal of Geosciences **5**, 1289-1295 (2012). DOI: https://doi.org/10.1007/s12517-010-0278-z

[14] J. Qiu, X. Li, R. Ge, S. Zhang, H. Wang, Formation mechanism of wire bow and its influence on diamond wire saw process and wire cutting capability. International Journal of Mechanical Sciences **185**, 105851 (2020). DOI: https://doi.org/10.1016/j.ijmecsci.2020.105851

[15] W.Y. Lee, K.W. Kim, H.C. Sin, Design and analysis of a milling cutter with the improved dynamic characteristics, International Journal of Machine Tools and Manufacture **42**, 8, 961-967 (2002). DOI: https://doi.org/10.1016/S0890-6955(02)00018-4

[16] Ch. Zhang, J. Zhang, On-line tool wear measurement for ball-end milling cutter based on machine vision, Computers in Industry **64**, 6, 708-719 (2013). DOI: https://doi.org/10.1016/j.compind.2013.03.010

[17] S. Yasar, A.O. Yilmaz, Rock cutting tests with a simple-shaped chisel pick to provide some useful data. Rock. Mech. Rock. Eng. **50**, 3261-3269 (2017). DOI: https://doi.org/10.1007/s00603-017-1303-2

[18] M. Klaic, Z. Murat, T. Staroveski, D. Brezak, Tool wear monitoring in rock drilling applications using vibration signals. Wear **408-409**, 222-227 (2018). DOI: https://doi.org/10.1016/j.wear.2018.05.012

[19] M. Khoshouei, R. Bagherpour, H. Sadeghisorkhani, M.H. Jalalian, A new look at hard rock abrasivity evaluation using acoustic emission technique (AET). Rock. Mech. Rock. Eng. **55**, 2425-2443 (2022). DOI: https://doi.org/10.1007/s00603-022-02787-x

[20] S. Nahak, S. Dewangan, S. Chattopadhyaya, G. Królczyk, S. Hloch, Discussion on importance of tungsten carbide – cobalt (WC-CO) cemented carbide and its critical characterization for wear mechanisms based on mining applications. Archives of Mining Sciences **63**, 1, 229-246 (2018). DOI: https://doi.org/10.24425/118897

[21] G. Straffelini, Friction and Wear: Methodologies for Design and Control. Springer Press, Berlin/Heidelberg (2016).

[22] K. Krauze, K. Mucha, T. Wydro, E. Pieczora, Functional and operational requirements to be fulfilled by conical picks regarding their wear rate and investment costs. Energies **14**, 3696 (2021). DOI: https://doi.org/10.3390/en14123696

[23] Bellator, 2024: BELLATOR Maszyny Budowlane Sp. z o.o. https://bellator-mb.pl/ (accessed 2 July 2024).

[24] H. Rafezi, F. Hassani, Drill bit wear monitoring and failure prediction for mining automation. International Journal of Mining Science and Technology **33**, 3, 289-296 (2023). DOI: https://doi.org/10.1016/j.ijmst.2022.10.006

[25] ISG, 2024: ISG Industrial Systems Group www.isg.com.sa (accessed 21 July 2024).

[26] Trow & Holden, 2024: Trow & Holden Company, Inc. https://trowandholden.com (accessed 21 July 2024).

[27] PN-EN 12058:2015-04 Natural stone products – Slabs for floors and stairs – Requirements (2015).

[28] PN-EN 1342:2013-05 Setts of natural stone for external paving – Requirements and test methods (2013).

[29] F. Kong, J. Xue, J. Shang, Ch. Zhu, M. Han, Z. Qu, B. Wang, K. Yang, Predicting uniaxial compressive strength of building stone based on index tests: Correlations, validity, reliability, and unification. Construction and Building Materials **438**, 137227 (2024). DOI: https://doi.org/10.1016/j.conbuildmat.2024.137227

[30] J.A. Valido, J.M. Cáceres, L. Sousa, Mechanical properties of ignimbrites of Tenerife Island employed as building stone and their correlation with some physical properties. Journal of Building Engineering **82**, 108222 (2024). DOI: https://doi.org/10.1016/j.jobe.2023.108222

[31] Y. Zhao, B. Liu, Ch. Wang, J. Bi, Z. Yang, Study on deterioration mechanism of granite with a natural single weak surface after freeze-thaw treatment. Cold Regions Science and Technology **218**, 104079 (2024). DOI: https://doi.org/10.1016/j.coldregions.2023.104079

[32] I. Tomašić, D. Lukić, N. Peček, A. Kršinić, Dynamics of capillary water absorption in natural stone. Bull. Eng. Geol. Environ. **70**, 673-680 (2011). DOI: https://doi.org/10.1007/s10064-011-0355-x

[33] G. Búrdalo-Salcedo, I. Rodríguez, M. Fernández-Raga, S. Fernández-Raga, C. Rodríguez-Fernández, J.M. González-Domínguez, Adaptation of a standard method for water Absorption testing of stone materials: The case of a hydrophilic protective coating. Materials **16**, 4228 (2023). DOI: https://doi.org/10.3390/ma16124228

[34] K. Mucha, Application of rock abrasiveness and rock abrasivity test methods – A review. Sustainability **15**, 11243 (2023). DOI: https://doi.org/10.3390/su151411243

[35] Cerchar – Centre d'Etudes et Recherches der Charbonnages de France, The Cerchar Abrasivity Index. Verneuil, 12 (1986).

[36] A.H. Deliormanlı, Cerchar abrasivity index (CAI) and its relation to strength and abrasion test methods for marble stones. Constr. Build. Mater. **30**, 16-21 (2012). DOI: https://doi.org/10.1016/j.conbuildmat.2011.11.023

[37] T.Y. Ko, T.K. Kim, Y. Son, S. Jeon, Effect of geomechanical properties on Cerchar Abrasivity Index (CAI) and its application to TBM tunnelling. Tunn. Undergr. Space Technol. **57**, 99-111 (2016). DOI: https://doi.org/10.1016/j.tust.2016.02.006

[38] M. Alber, Stress dependency of the Cerchar abrasivity index (CAI) and its effects on wear of selected rock cutting tools. Tunnelling and Underground Space Technology **23**, 4, 351-359 (2008). DOI: https://doi.org/10.1016/j.tust.2007.05.008

[39] M. Khoshouei, M.H. Jalalian, R. Bagherpour, The effect of geological properties of dimension stones on the prediction of specific energy (SE) during diamond wire cutting operations. Rudarsko-geološko-naftni zbornik **35**, 3 (2020). DOI: https://doi.org/10.17794/rgn.2020.3.2

[40] M.V. Ozdogan, A.H. Deliormanli, H. Yenice, The correlations between the Cerchar Abrasivity Index and the geomechanical properties of building stones. Arab. J. Geosci. **11**, 604 (2018). DOI: https://doi.org/10.1007/s12517-018-3958-8

[41] A.Z. Abu Bakar, Y. Majeed, J. Rostami, Effects of rock water content on CERCHAR Abrasivity Index. Wear **68-369**, 132-145 (2016). DOI: https://doi.org/10.1016/j.wear.2016.09.007

[42] Ch. Yan, G. Li, W. Zhan, Q. Li, G. Yang, J. Yang, G. Gao, Water saturation effects on rock abrasivity and TBM tunneling efficiency. Wear **538-539**, 205236 (2024). DOI: https://doi.org/10.1016/j.wear.2024.205236

[43] M. Suana, T. Peters, The Cerchar Abrasivity Index and its relation to rock mineralogy and petrography. Rock Mechanics **15**, 1-8 (1982). DOI: https://doi.org/10.1007/bf01239473

[44] C. Dogruoz, Cerchar Abrasivity Index Prediction Using Multi-Proxy Data. A Case Study from the Sagdere Formation (Denizli Molasse Basin, Turkey). Archives of Mining Sciences **65**, 4, 787-801 (2020). DOI: https://doi.org/10.24425/ams.2020.134147

[45] S. Er, M. Yilmaz, A. Ertin, A. Tugrul, N. Tokgöz, Assessment of excavatability, abrasivity and slope stability in a sandstone quarry in Istanbul. Turkey. J. Geol. Soc. India. **89**, 581-588 (2017). DOI: https://doi.org/10.1007/s12594-017-0647-2

[46] S. Kahraman, M. Alber, M. Fener, O. Gunaydin, The usability of Cerchar Abrasivity Index for the prediction of UCS and E of Misis Fault Breccia: Regression and artificial neural networks analysis. Expert Systems with Applications **37**, 12, 8750-8756 (2010). DOI: https://doi.org/10.1016/j.eswa.2010.06.039

[47] E. Khoshzaher, H. Chakeri, M. Darbor, H. Shakeri, The effects of water content and grain size on the clogging and abrasivity of fine-grained soils in mechanized excavation. Rudarsko-geološko-naftni zbornik **38**, 2, 65-74 (2023). DOI: https://doi.org/10.17794/rgn.2023.2.4

[48] H. Jeong, S. Choi, Y.K. Lee, Evaluation of cutting performance of a TBM disc cutter and Cerchar Abrasivity Index based on the brittleness and properties of rock. Appl. Sci. **13**, 2612 (2023). DOI: https://doi.org/10.3390/app13042612

[49] J. Rostami, A. Ghasemi, E.A. Gharahbagh, C. Dogruoz, F. Dahl, Study of dominant factors affecting Cerchar Abrasivity Index. Rock. Mech. Rock. Eng. **47**, 1905-1919 (2014). DOI: https://doi.org/10.1007/s00603-013-0487-3

[50] K. Mucha, The new method for assessing rock abrasivity in terms of wear of conical picks. New Trends Prod. Eng. **2**, 186-194 (2019). DOI: http://dx.doi.org/10.2478/ntpe-2019-0019

[51] P. Strzałkowski, U. Kaźmierczak, M. Wolny, Assessment of the method for abrasion resistance determination of sandstones on Böhme abrasion test apparatus. Bulletin of Engineering Geology and the Environment **79** (9), 4947-4956 (2020). DOI: https://doi.org/10.1007/s10064-020-01868-x

[52] A.A.A. Mohammed, M. Fener, R. Comakli, I. Ince, M.C. Balci, K. Kayabalı, Investigation of the relationships between basic physical and mechanical properties and abrasion wear resistance of several natural building stones used in Turkey. Journal of Building Engineering **42**, 103084 (2021). DOI: https://doi.org/10.1016/j.jobe.2021.103084

[53] I. Çobanoğlu, S.B. Çelik, Assessments on the usability of Wide Wheel (Capon) test as reference abrasion test method for building stones. Construction and Building Materials **151**, 319-330 (2017). DOI: https://doi.org/10.1016/j.conbuildmat.2017.06.045

[54] A. Teyman, The usability of Cerchar Abrasivity Index for the estimation of mechanical rock properties. International Journal of Rock Mechanics and Mining Sciences **128**, 104258 (2020). DOI: https://doi.org/10.1016/j.ijrmms.2020.104258

[55] PN-EN 1936:2010 Natural stone methods – Determination of real density and apparent density and total open porosity (2010).

[56] PN-EN 13755:2008 Natural stone test methods – Determination of water absorption at atmospheric pressure (2008).

[57] PN-EN 1926:2007 Natural stone test methods – Determination of compressive strength (2007).

[58] PN-EN 14157:2017-11 Natural stone test methods – Determination of abrasion resistance (2017).

[59] Q. Li, J. Li, L. Duan, S. Tan, Prediction of rock abrasivity and hardness from mineral composition. International Journal of Rock Mechanics and Mining Sciences **140**, 104658 (2021). DOI: https://doi.org/10.1016/j.ijrmms.2021.104658

[60] N. Gunes Yılmaz, R.M. Goktan, T. Onargan, Correlative relations between three-body abrasion wear resistance and petrographic properties of selected granites used as floor coverings. Wear **372-373**, 197-207 (2017). DOI: https://doi.org/10.1016/j.wear.2016.12.024